Vibrio fischeri and *Escherichia coli* adhesion tendencies towards photolithographically modified nanosmooth poly (*tert*-butyl methacrylate) polymer surfaces

Elena P Ivanova[1]
Natasa Mitik-Dineva[1]
Radu C Mocanasu[1]
Sarah Murphy[1]
James Wang[2]
Grant van Riessen[3]
Russell J Crawford[1]

[1]Faculty Life and Social Sciences; [2]IRIS, Swinburne University of Technology, Hawthorn, Victoria, Australia; [3]Centre for Materials and Surface Science, La Trobe University, Melbourne, Victoria, Australia

Abstract: This study reports the adhesion behavior of two bacterial species, *Vibrio fischeri* and *Escherichia coli*, to the photoresistant poly(*tert*-butyl methacrylate) (P(*t*BMA)) polymer surface. The data has demonstrated that ultraviolet irradiation of P(*t*BMA) was able to provide control over bacterial adhesion tendencies. Following photolithography, several of the surface characteristics of P(*t*BMA) were found to be altered. Atomic force microscopy analysis indicated that photolithographically modified P(*t*BMA) (henceforth termed 'modified polymer') appeared as a 'nanosmooth' surface with an average surface roughness of 1.6 nm. Although confocal laser scanning microscopy and scanning electron microscopy analysis clearly demonstrated that *V. fischeri* and *E. coli* presented largely different patterns of attachment in order to adhere to the same surfaces, both species exhibited a greater adhesion propensity towards the 'nanosmooth' surface. The adhesion of both species to the modified polymer surface appeared to be facilitated by an elevated production of extracellular polymeric substances when in contact with the substrate.

Keywords: poly(*tert*-butylmethacrylate) polymeric surfaces, surface nanotopography, bacterial attachment, extracellular polymeric substances

Introduction

The pioneering research of Henrici and Zobell (Zobell and Allen 1935; Zobell 1937; Zobell 1942) recognized the importance of surface-attached bacteria almost 80 years ago. The solid/liquid interface between a surface and an aqueous medium has been seen to be a common location for biofilm formation. This can cause contamination in areas as diverse as dentistry (eg, formation of plaque) (Busscher and van der Mei 1997; Marsh and Bradshaw 1997), biomedicine (eg, implants and other biopolymers) (Gristina et al 1993; Hendricks et al 1999), and water treatment facilities (Percival et al 2000). This solid/liquid interface becomes almost immediately conditioned from the aqueous medium, in which it is immersed, resulting in a chemical or physical modification which is thought to aid in bacterial attachment (Loeb and Neihof 1975). Despite numerous studies being undertaken, this process remains poorly understood, primarily because of the vast variety of surface properties possessed by both the bacterial cells and surface of the substrata (Characklis 1973; Reynolds and Wong 1983; Hogt et al 1985; Pringle and Fletcher 1986; Oga et al 1988; Barth et al 1989; An and Friedman 1998; Liang et al 2000; Tegoulia and Cooper 2002). Characteristics such as surface hydrophobicity, surface charge, and surface chemical composition together with the physiological cell features such as fimbriae, pili, extracellular polymeric substances, and cellular surface charge have been shown to affect the adherence of cells. Most of these issues have been addressed in several excellent reviews on bacterial biofilm formation, structure and function (Handley et al

Correspondence: Elena P Ivanova
Swinburne University of Technology,
PO Box 218, Hawthorn, Victoria 3122,
Australia
Tel: +613-92145137
Fax: +613-92145050
Email: eivanova@swin.edu.au

2001; Davey and O'Toole 2000; Donlan 2002; Stoodley et al 2002; Weibel et al 2007).

Nonspecific cell to surface interactions have been explained by a number of physicochemical interactions including van der Waals, electrostatic interactions, and hydrophobic interactions (Fletcher 1996; Busscher et al 1999; Li and Logan 2004; Senaratne et al 2005). There is, however, currently no complete model to explain the attachment of bacterial cells from different taxonomic groups to a surface. Several studies have indicated that some of the following factors influence the adhesion of some species to a surface: the chemical compositions of the surface itself (Oga et al 1988; Barth et al 1989), the bacterial cell surface electrokinetic properties (Li and Logan 2004) and the surface charge of the substratum (Hogt et al 1985). Hydrophobicity (Reynolds and Wong 1983; Pringle and Fletcher 1986) and simple surface roughness or physical configuration (An et al 1995) have also been identified as influential factors. Electrokinetic properties have previously been shown to play a fundamental role in bacterial aggregation (Eboigbodin et al 2005). Marshall (1984) proposed that electrokinetic properties were a major factor in the attraction or repulsion of bacterial cells to surfaces. Several studies have indicated that bacterial adhesion negatively correlated with bacterial zeta potentials (van Loosdrecht et al 1989; Tsuneda et al 2003; Li and Logan 2004; Tsuneda et al 2004; Eboigbodin et al 2005), conversely, other studies have been reported that there are no relationship between the two parameters (Abbot et al 1983; Hogt et al 1985; Harkes et al 1991). A review by Donlan (2002) has discussed the contribution of bacterial fimbriae in the surface attachment mechanism. The presence of such features are thought to positively influence adhesion by reducing the initial electrostatic barrier to adsorption that can exist between the cell and surface by increasing the cell surface hydrophobicity. Other proteins, extracellular polysaccharides and flagella are also thought to play an important role in the attachment process (Donlan 2002).

Recently, the issue of gaining control over nonspecific binding interactions has received a significant amount of attention, in particular in the course of the development of novel nanofabrication techniques (An et al 1995; Li and Logan 2004). A range of studies in bio- and nanotechnology have begun to bridge the gap between biologists who study microbial life and physical scientists/engineers who manufacture new materials and structures. A review by Weibel and colleagues (2007) addressed the significant union of these technologies. The size scale in nanotechnology studies is well matched to the physical dimensions of most microorganisms, allowing the possibility to manipulate the microenvironment of cells as well as the individual cells themselves. In order to create useful substrata for biotechnological applications it is essential to address both the enhancement of specific binding and the reduction of nonspecific binding of biological systems to an interface. A reduction in nonspecific binding alone would have a great impact on many areas of biotechnology (Busscher and van der Mei 1997; Marsh and Bradshaw 1997).

The current study employs a polymer, photoresistant poly(*tert*-butyl methacrylate) (P(*t*BMA)), commonly used in biomedical applications, to investigate the factors that may control the nonspecific attachment of two bacterial species, *Escherichia coli* and *Vibrio fischeri.* P(*t*BMA) substrates were selected as sample surfaces because of its exceptional mechanical and optical characteristics (transparency, stiffness, low water absorption, high abrasion resistance, etc) for which P(*t*BMA) has been frequently used as a positive photoresist. Currently no published data is available on the attachment mechanisms of *E. coli* and *V. fischeri* specifically to P(*t*BMA) and/or modified P(*t*BMA) polymer surfaces. Moreover, there is no complete model to explain the attachment of bacterial cells from different taxonomical groups to a variety of substrates. In this context, the aim of this study was to study the nonspecific interactions of the two bacterial species, *E. coli* and *V. fischeri* at the interface of the P(*t*BMA) polymer surface before and after surface modification using ultraviolet (UV) photolithography. Cell-surface interactions were assessed using a variety of techniques including scanning electron microscopy (SEM), atomic force microscopy (AFM), confocal laser scanning microscopy (CLSM), contact angle, and cellular surface charge measurements.

Material and methods

Polymeric surface preparation

Poly(*tert*-butyl methacrylate) (P(*t*BMA); Sigma-Aldrich, St. Louis, MO, USA) was used as the polymer substrate. The substrates were prepared as described elsewhere (Ivanova et al 2006). Briefly, a 4 wt% solution of P(*t*BMA) (MW~170,000) in propylene glycol methyl ether acetate (PGMEA) (Sigma Aldrich) 99% was used. Polymer films were prepared on 22 × 60 mm glass substrates (glass cover slips, 1 oz, Deckgläser) that were previously sonicated in isopropanol (Pr_iOH) for 30 min, washed with copious amounts of sterile nanopure H_2O (18.2 $M\Omega cm^{-1}$ Barnstead/Thermolyne NANOpure Infinity water purification system), and dried under a stream of high purity nitrogen prior

to priming with hexamethyldisilazane (HMDS) (Sigma Aldrich). Primer was spun at 1000 rpm for 15 seconds and polymers at 3000 rpm for 40 seconds using a spin coater (Model P6708; Specialty Coating Systems, Indianapolis, IN, USA). Finally, polymer covered slides were post-exposure baked for 60 minutes at 95 °C and stored in a desiccator prior to use.

Photolithography was carried out as described elsewhere (Ivanova et al 2006). The native P(*t*BMA) substrates, prepared as described above, were then UV- exposed (254 nm, 760 μW cm^{-2}) for 10 minutes. The UV-irradiated samples were post-exposure baked at 90 °C for 20 minutes to facilitate diffusion of the photogenerated acid thereby initializing *tert*-butyl ester deprotection. All samples were dried at room temperature and stored in a desiccator prior to use.

Contact angle measurements

Advancing contact angles were measured using sessile drops (2 μL) of nanopure water at room temperature (20–23 °C) in air using a contact angle meter constructed from an XY stage fitted with a (20 μL) micro syringe, a 20 × magnification microscope (Isco-Optic, Goettingen, Germany) and a fiber-optic illuminator. The images were captured using a digital camera (AIPTEK Inc., Hsinchu, Taiwan), and analyzed using PaintShop Pro (Jasco Software, Fremont, CA, USA). Final contact angles were taken as the average of six different measurements.

Bacterial cell surface hydrophobicity was evaluated from contact angles measurements on lawns of bacteria using the sessile drop method. Bacterial cells in a buffer ($OD_{(600)} = 0.4$) were deposited on cellulose acetate membrane filters (Sartorius, 0.2 μm). The wet filters were air dried at ambient temperature (ca. 22 °C) for approximately 30–40 minutes to air dry until a "plateau state". Water droplets were deposited on each surface. The drop was allowed to settle for 2 seconds without needle contact (for static contact angle measurements). Images were digitally saved. Contact angle values were obtained by processing the image with the instrument software.

Surface characterization by atomic force microscopy

A scanning probe microscope (SPM) (Solver P7LS, NT-MDT) was used to image the surface morphology and to quantitatively measure and analyze the surface roughness of both native and modified P(*t*BMA) on the nanometer scale. The analysis was performed in the semi-contact mode which reduces the interaction between tip and sample and thus allows the destructive action of lateral forces that exist in contact mode due to be avoided. The carbon "whisker" type silicon cantilevers (NSC05, NT-MDT) with a spring constant of 11 N/m, tip radius of curvature of 10 nm, aspect ratio of 10:1 and resonance frequency of 150 KHz were used to obtain good topographic resolution. Scanning was performed perpendicular to the axis of the cantilever at a typical rate of 1 Hz. Image processing of the raw topographical data was performed with first order horizontal and vertical leveling, and the topography and surface profile of the samples were obtained simultaneously. In this way the surface features of the samples were measured with a resolution of a fraction of nanometer and the surface roughness of the investigated areas could be statistically analyzed using the standard instrument software (LS7-SPM v. 8.58).

Bacterial strains

E. coli K12 was cultured on Luria-Bertani (LB) broth (Tryptone 10.0 g L^{-1}, yeast extract 5.0 g L^{-1}, NaCl 10.0 g L^{-1}, adjusted to pH 7.0) (Sambrook and Russell 2001) and LB Agar (as LB Broth with the addition of 1.5% Agar). Type strain *V. fischeri* DSM 507^T was obtained from the DSMZ (Microbial Culture Collection, Germany). *V. fischeri* was routinely cultured on Marine Agar 2216 (Difco). Both strains were incubated at room temperature (ca 22 °C) and stored at −80°C in Marine Broth 2216 (Difco) or LB Broth supplemented with 20% (v/v) of glycerol.

Cellular surface charge measurements

Zeta potential measurements of both *V. fischeri* and *E. coli* were obtained by measuring the electrophoretic mobility (EPM) as described elsewhere (de Kerchove and Elimelech 2005). The EPM was measured as a function of ionic strength by microelectrophoresis using the Zeta Potential Analyser (ZetaPALS, Brookhaven Instruments Corp, Holtsville, NY). The bacterial cell suspension was freshly prepared before the measurement. After 24 h of growth in marine broth, the cells were harvested by centrifugation for 5 min at 5000 rpm. Harvested cell pellet was re-suspended in 10 mM potassium chloride (KCl) followed by further washing and centrifugation. This step was repeated four times to eliminate residual extracellular polysaccharides as these may influence the surface electric potential. After the final wash, cell pellets were re-suspended in 10 mM KCl solution to $OD_{(600nm)} = 1$ (de Kerchove and Elimelech 2005). This cell solution was then diluted 1000 times in 5 mL of 10mM KCl for the EPM measurements. Measurements were conducted in electric

field 2.5 V cm^{-1} and 2 Hz (Eboigbodin et al 2006). All measurements were done in triplicate and for each sample the final EPM quoted represented the average of 5 successive ZetaPALS readings, each of which consisted of 14 cycles per run. All data was processed using the accompanied software employing the Smoluchowski equation (de Kerchove and Elimelech 2005; Eboigbodin et al 2005).

Bacterial growth and sample preparation

Both bacterial species were applied individually to both the native and modified P(*t*BMA) surfaces. Bacterial species were incubated with the appropriate media and temperature to reach a cell density of OD_{600} 0.40 ± 0.05. Polymer coated glass cover slides were placed in a sterile Petri-dish in duplicate. The Petri-dish was inoculated with 5 mL of log-phase culture, to submerge the slides. Petri dishes were incubated overnight (12 h) at room temperature (ca. 22 °C). On the following morning all slides were rinsed three times with sterilized nanopure H_2O (18.2 MΩcm^{-1}), left to air-dry under sterile conditions on ambient temperature without additional fixation to prevent deformation of the cells and were further processed. Sterile marine broth 2216 (5 mL) was used as a negative control. Three independent experiments were performed for each polymeric surface. Both LB broth and marine broth 2216 were used throughout all experiments as negative controls in order to verify that the medium used did not have the ability to leave any deposits that visually appear like cells or EPS.

Visualization of viable cells and EPS

In order to visualize viable bacterial cells attached to the polymer surface as well as the production of extracellular substances in the process of adhesion two dyes were used simultaneously. Concanavalin A Alexa Fluor 488 Conjugate (Molecular Probes, Carlsbad, CA, USA) was applied in order to visualize EPS. This dye selectively binds to α-mannopyranosyl and α-glucopyranosyl residues in EPS (Goldstein et al 1964). Concanavalin A stock solution was prepared by dissolving 5 mg in 5 mL of 0.1 M sodium bicarbonate at pH 8.3 and stored at 20 °C. The working solution was prepared by diluting stock solution to 1:20 using the same buffer to avoid changes in pH. According to the manufacturer protocol, the excitation and emission wavelengths for Concanavalin A are 495 and 519 nm, respectively.

The Vybrant CFDA SE Cell Tracer Kit (Invitrogen, Carlsbad, CA, USA) was used to trace viable cells adsorbed on each of the surfaces. The kit contains CFDA SE (carboxyfluorescein diacetate, succinimidyl ester) that is initially colorless and nonfluorescent. It passively diffuses into cells where the acetate groups are cleaved by intracellular esterases to yield highly fluorescent, amine-reactive carboxyfluorescein succinimidyl ester. The dye–protein adducts that form in labeled cells are retained by the cells and inherited by daughter cells after division. The excitation and emission wavelengths for CFDA SE are 4952 and 517 nm, respectively. Working solutions of the dye as well as cell labeling conditions were prepared as described elsewhere (Invitrogen 2006). In general the P(*t*BMA) substrates were incubated in the bacterial suspension for 11h before an aliquot of Concanavalin A 488 was added in ratio 1:5 (cell suspension/dye). The dye was allowed 1h to diffuse when CFDA SE dye, in the same ratio, was added to the suspension and incubated for additional 15 min at 37 °C.

After incubation, the samples were washed with sterilized nanopure H_2O (18.2 MΩcm^{-1}), left to dry for several hours at room temperature (ca. 22 °C, humidity 48%) without additional fixation to prevent the deformation of the cells and processed on the following day using confocal microscopy. The CSLM used was the Olympus FluoView™ FV1000 Spectroscopic Confocal System which included an inverted Microscope System OLYMPUS IX81 (20X, 40X (oil), 100X (oil) UIS objectives) which operates using multi Ar and HeNe lasers (458, 488, 515, 543, 633 nm). The system is equipped with a transmitted light differential interference contract attachment and a CCD camera (Cool View FDI).

Scanning electron microscopy

High resolution images of the bacterial cell attachment to the polymeric surfaces were obtained using a FeSEM instrument (Model ZEISS SUPRA 40VP). The samples were air-dried on ambient temperature for 1 hour and sputter-coated with gold prior to imaging. Primary beam energies of 3 to 15 kV were used, allowing observation of features on the sample surface or within a few microns of the surface, respectively.

SEM images enabled quantitative as well as qualitative cell analyses. For quantification of the number of adsorbed bacteria, cells number from at least ten representative images/areas was transformed into number of bacteria per unit area using the Image-Pro software (Waar et al 2002). The final densities have estimated errors of approximately 10%–15% due to local variability in the coverage.

Results

Polymer surface characterization

Contact angle measurements and AFM analysis were applied to the native and modified P(*t*BMA) surfaces in

order to identify the effects of the modification process on the polymer surface characteristics. Surface hydrophobicity was determined using advancing contact angle measurements with two diagnostic liquids, water and glycerol (Table 1). The modified P(*t*BMA) surface was found to be moderately less hydrophobic (a contact angle of approximately 64°) than the native P(*t*BMA) (a contact angle of approximately 87°). A small reduction of glycerol contact angle was also observed (from 79° to approximately 72°). The surfaces modification resulted in change of surface chemistry where the presence of carboxylic groups was confirmed by the XPS analysis. These results are in concordance with already reported wettability for P(*t*BMA) (Ivanova et al 2006).

AFM analysis of both native and modified P(*t*BMA) indicated a topographical alteration in surface roughness on the nanometer scale. An increase in the uniformity of P(*t*BMA) surface topographical features was observed after UV exposure, as shown on Figure 1. Figure 1a represents the topography of the native P(*t*BMA) on a nanometer scale, where a colour variation is noted across the field of view, indicating nonuniform high peaks (approx 40–50 nm) and low valleys (0–5 nm) across the polymer surface. The transverse profile in conjunction with the calculated roughness data confirmed nanoscale variation in surface height (Table 1). In contrast to the native polymer, the topographical image of modified P(*t*BMA) shown in Figure 1b displayed more uniform surface characteristics. Peak heights of max 11–20 nm were observed that were two to four times less than the peak height observed on the native polymer. These results suggest that the native P(*t*BMA) is approximately twice as rough (on the nanometer scale) as the modified P(*t*BMA).

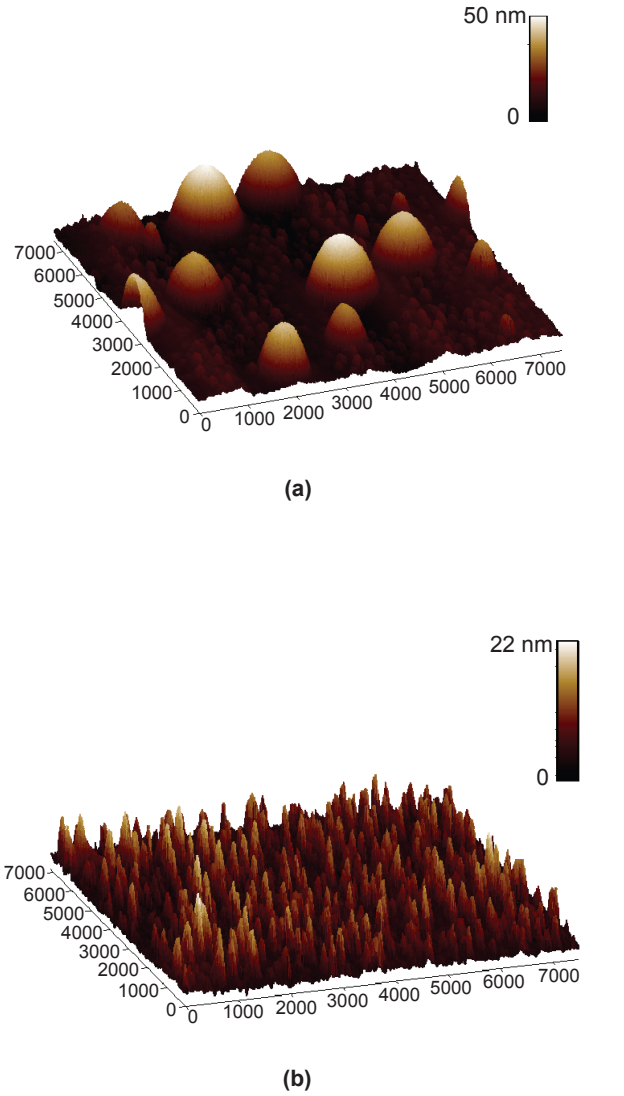

Figure 1 Typical 3D AFM images of the P(*t*BMA) surfaces as received (**a**) and after UV exposure (**b**) showing the surface roughness transformation after UV exposure.

Bacterial cell surface characterization

Electrophoretic mobility (EPM) is a commonly used technique for surface characterization of nonbiological colloids and, more recently, bacterial cells (Tsuneda et al 2003; de Kerchove and Elimelech 2005; Eboigbodin et al 2005, 2006). Cell surface electrokinetic properties are implied from the measurement of the movement of the charged particles eg, cell, in an external electric field to obtain the EPM. The magnitude of the EPM gives an indication of the overall net charge on the surface of a particle where; a negative EPM value indicates that a particle has a negative charge, while a positive EPM value indicates that the particle has a net positive charge (de Kerchove and Elimelech 2005; Eboigbodin et al 2005). Through the application of Smoluchowski's equation EPM is related to the zeta potential, where zeta potential is assumed to be equal to the cellular surface charge (Masliyah 1994; Hunter 1995). Zeta potential measurements were performed in order to characterize the electrokinetic surface properties of each bacterium. The observed cellular surface charge of *V. fischeri* and *E. coli* are shown in Table 2. *V. fischeri* and *E. coli* exhibited zeta potentials from

Table 1 Wettability and surface roughness analysis of the P(*t*BMA) surfaces

P(*t*BMA)	Contact Angle, Θ		Surface roughness (nm)		
	Water (°)	Glycerol (°)	Ra	Rq	Rmax
As received	86.5 ± 1.5	79.8 ± 3.0	5.25	8.55	53.65
Modified	63.5 ± 3.0	72.5 ± 3.5	1.56	2.36	21.46

Table 2 Electrophoretic mobility, zeta potential and surface wettability of *V. fischeri* and *E. coli*

Species	Electrophoretic mobility, (μs^{-1} Vcm^{-1})	Zeta potential, (mV)	Surface wettability (θ), water (°)
V. fischeri	–2.4 ± 0.7	–30.1 ± 9	83.2 ± 5
E. coli	–3.0 ± 0.2	–38.4 ± 3	33.0 ± 4

approximately –30 ± 9 mV to –38 ± 3 mV, highlighting that both species possess negative charge at pH 7.2 with *E. coli* displaying a slightly more negative charge than *V. fischeri*. It was also found that the *E. coli* cells surface was less hydrophobic in the range of θ = 33.0° ± 4°, while *V. fischeri* cells surface was highly hydrophobic, θ = 83.2° ± 5°.

Attachment pattern of *V. fischeri* and *E. coli*

CSLM images of *V. fischeri* attached to both native and modified P(*t*BMA) are presented in Figure 2. Figure 2a shows the production of EPS by *V. fischeri* cells attached to the native P(*t*BMA) surface. It is evident that attached cells typically gathered in areas of moderate cell density. The image also suggests that the EPS produced by cells adsorbed on this surface is capsular EPS as each cell appears to be individually enveloped. The use of CFDA SE cell viability assay indicated that cells not only successfully attached but also were capable of maintaining their viability (Figure 2b).

The attachment of viable *V. fischeri* cells on modified P(*t*)BMA is observed in Figure 2d. It is also evident that apart from the sessile cells evenly distributed over the entire surface, organized multi-cellular clusters were also present. Granular-like deposits (circled areas) on the polymer surface were also observed (Figure 2c).

CSLM images of *E. coli* cell attachment to both of the polymeric surfaces presented in Figure 3. As it can be seen from Figure 3a, only several *E. coli* cells attached to the surface of native P(*t*BMA) suggesting that this species was not able to successfully colonize this polymeric surface.

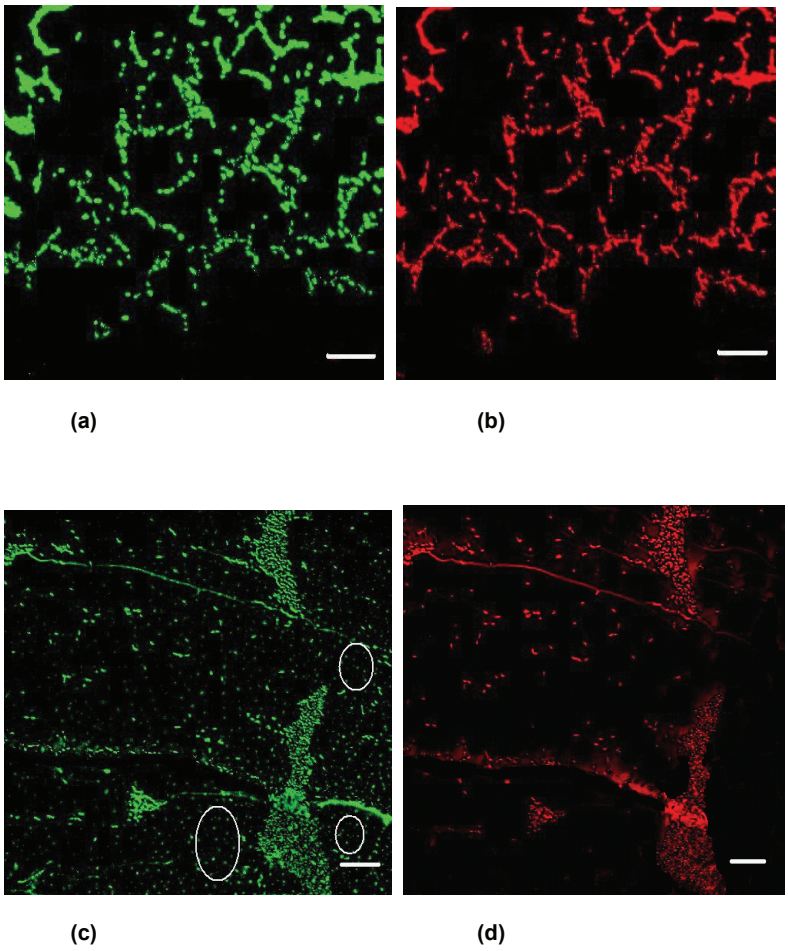

Figure 2 CLSM images displaying *V. fischeri* cell viability (**b**, **d**) and the production of EPS (a, c) on the as received P(*t*BMA) (**a**, **b**) and modified polymer surface (**c**, **d**). Circled areas indicate the presence of EPS deposited on the surfaces. The scale bar represents 10 μm on all images.

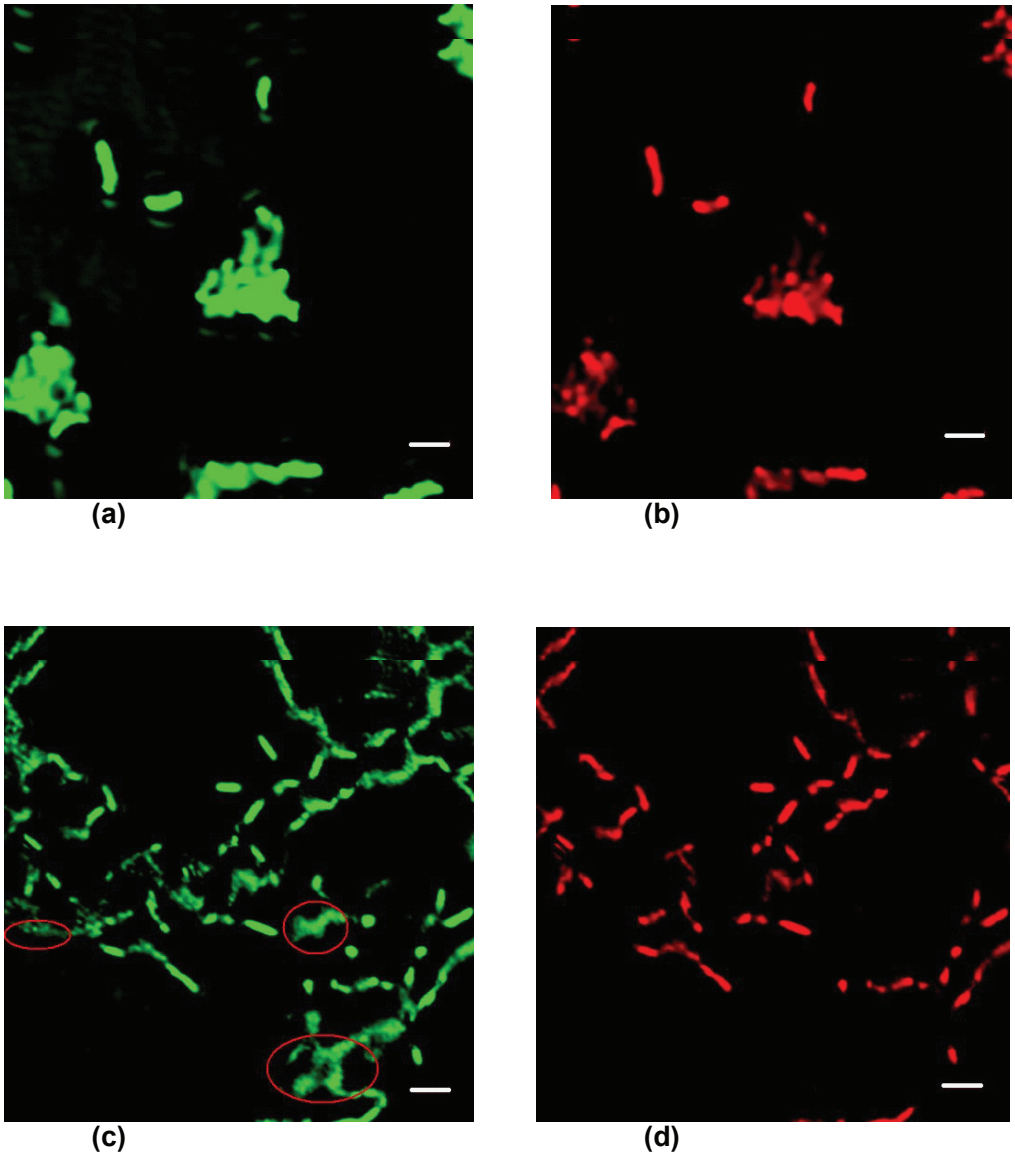

Figure 3 CLSM images displaying *E. coli* cell viability (**b**, **d**) and the production of EPS (a, c) on the as received P(*t*BMA) (**a**, **b**) and modified polymer surface (**c**, **d**). Circled areas indicate the presence of EPS deposited on the surfaces. The scale bar represents 5μm on all images.

It is very difficult to distinguish any viable cells or EPS by fluorescence in the accompanying image (Figure 3b). CSLM images presented in Figures 3c, 3d show that in contrast to native P(*t*BMA), a considerable number of *E. coli* cells were able to attach to the surface of the modified polymer. *E. coli* cells appeared in clusters where the majority of the cells were viable (red colored) as inferred from the cell viability assay. It can be seen that appreciable quantities of EPS are encapsulating the bacterial cells.

Due to the limitations of optical microscopy, SEM was employed in order to study the bacterial attachment pattern and cellular morphology while adhering to the polymer surfaces. SEM images showing the attachment of *V. fischeri* to both native and modified P(*t*BMA) are presented in Figures 4a–4d. It can be seen from the SEM images that V. *fischeri* cells were able to colonize the moderately hydrophobic surface of native P(*t*BMA) (Figure 4a). However, a greater number of cells appear to have been able to successfully attach to the modified polymer surface. Cells are well defined and appeared healthy with noticeable flagella (Figure 4b). Surface colonization appears to be relatively even across the polymeric surface. Figure 4b shows the distribution of suspected EPS materials (white substance) produced by *V. fischeri*. It can be seen that the greatest quantities of EPS are present in areas where cells are within close proximity of one another. The number of cells

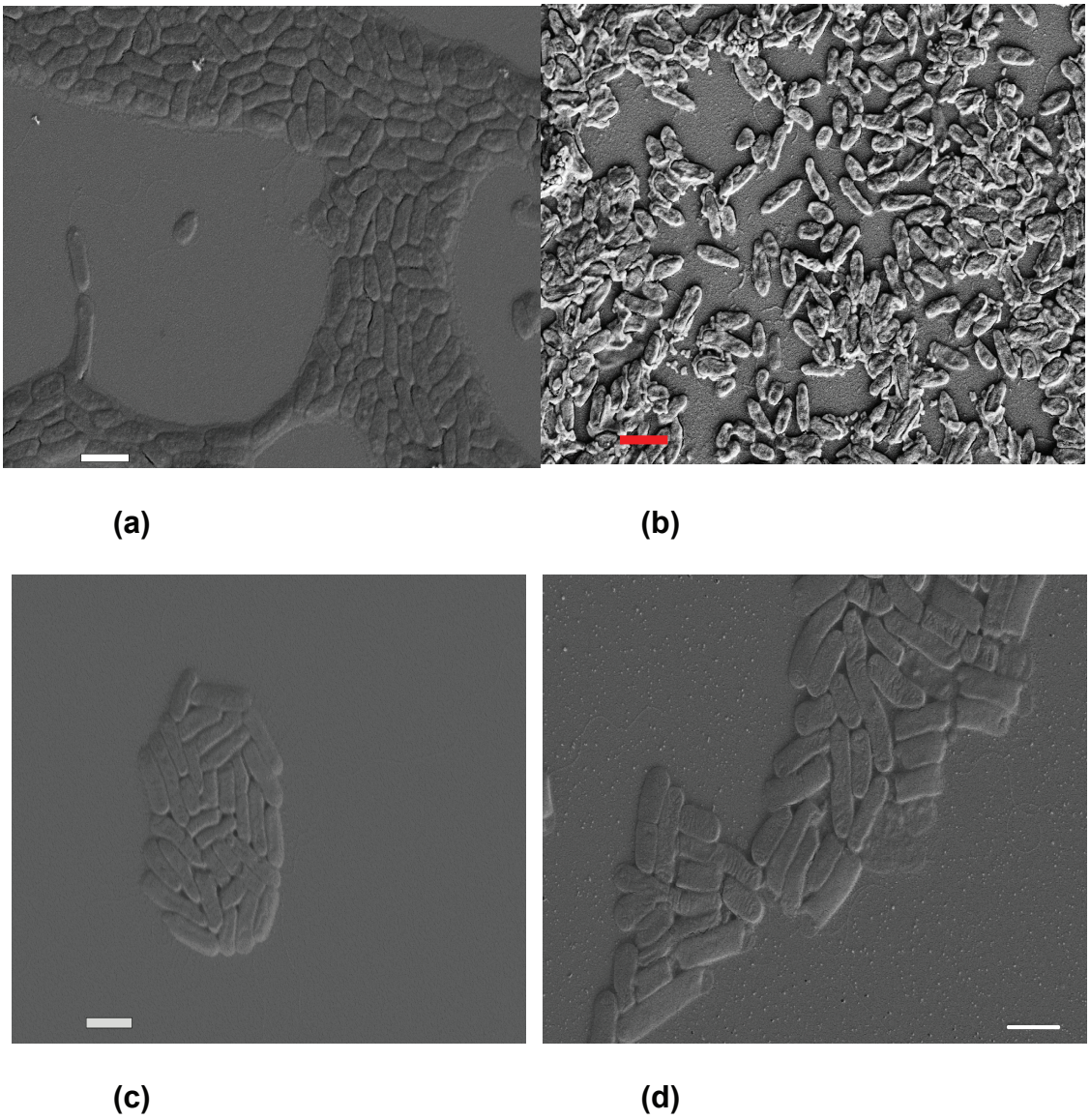

Figure 4 Typical attachment pattern of *V. fischeri* and *E. coli* cells on the P(*t*BMA) polymer surfaces, as received (**a**, **c**), and modified by photolithography (**b**, **d**) at 5000 × magnification. SEM images (**b**) and (**d**) indicate significant amount of EPS produced by the cells of *V. fischeri* in particular while attaching to modified P(*t*BMA). The scale bar is 2 μm.

adsorbed to each of the surfaces was roughly estimated at 10.97×10^6 cells/cm^2 ± 12% and 15.68×10^6 cells/cm^2 ± 12% to the native and to the modified P(*t*BMA), respectively.

Typical SEM images presented in Figures 4c, 4d illustrate the attachment behavior of *E. coli* cells to both, native (Figure 4c) and modified (Figure 4d) P(*t*BMA). In can be seen that the overall colonization of the modified P(*t*BMA) surface was greater when compared to the native. This visually attained observation was confirmed when the number of cells per mm^2 was calculated. It was roughly estimated that the overall number of *E. coli* cells attached to the native P(*t*BMA) was 3.1×10^6 cells per cm^2 ± 10%, with the overall length of the cells attached to the native polymer surface in the range of 1.5–2 μm. The number of cells attached to the modified polymer surface was significantly greater in the range of 7.6×10^6 cells per cm^2 ± 10%.

Discussion

Since there are a number of factors that can influence the initial bacterial attachment, the characteristics of polymer surfaces before and after UV-irradiation were investigated in detail. The photolithographic treatment of P(*t*BMA) resulted in the modification of a number of polymer surface characteristics such as hydrophobicity, surface chemistry and nanotopography. Modified P(*t*BMA) surfaces were found to be moderately less hydrophobic

(water contact angle 63° ± 3°) than the native polymer surfaces which is likely to be due to the loss of methyl groups and the *tert*butyl ester on the polymer backbone and the formation of carboxylic acid groups (Ivanova et al 2006). Observed water contact angles are consistent with previously reported values. Native P(*t*BMA) has been cited to have water contact angle values ranging from 77° (Ivanova et al 2006) to 91° (Pham et al 2003). Previous XPS analysis revealed conclusive evidence to support the premise that surface carboxylic acid groups are present on modified P*t*BMA polymer surface.

The surface roughness of P(*t*BMA) was also altered by UV-irradiation. The evaluated root-mean-square roughness (Rq) value of native P(*t*BMA) was seen to reduce from 8.5 nm to 2.4 nm after irradiation (the standard error for the surface roughness measurements was estimated in a range of 10%). The root-mean-square value is a statistical measure of the magnitude of a varying quantity, and has been employed in previous research to give an accurate indication of the varying topography of a surface (Pham et al 2003). The average and the maximum surface roughness, Ra and Rmax respectively, were also reduced from 5.5 nm and 53.65 nm on the native P(*t*BMA) to 1.6 nm and 21.46 nm on the modified P(*t*BMA) surface. These results indicated that the surface roughness of modified P(*t*BMA) was also altered as the surface appeared uniformly smoother without the relatively prominent high protrusions and is approximately half as rough as the native polymer.

Analysis of both CSLM and SEM images revealed striking differences in the bacterial responses to the native and modified P(*t*BMA) polymeric surfaces. Differentiation was observed in the number of attached bacterial cells and the extent of EPS production. The overall distribution of *E. coli* cells over both, the native and the modified surface, was significantly lower when compared to *V. fischeri*. Yet consistent trend of increased cellular presence on the modified polymer surface was observed for both strains. This observation is concordant with previous research, which observed bacterial adhesion to be negatively correlated with bacterial zeta potential (Li and Logan 2004), indicating that if one considers cellular surface charge alone, *V. fischeri* is more likely to take part in surface adhesion than *E. coli*.

Concanavalin A Alexa Fluor 488 Conjugate was able to highlight α-mannopyranosyl and α-glucopyranosyl residues apparently present in EPS in CSLM images for both species, suggesting that the EPS produced by both species contained these residues in their exopolysaccharides. It is noted, however, some visual difference in appearance of EPS produced by two strains studied. Several studies have addressed the characterization of EPS produced by different species (Wright et al 1990; Watnick and Kolter 1999; Yildiz and Schoolnik 1999; Sutherland 2001; Wozniak et al 2003). These studies have demonstrated that EPS can vary widely in composition, structure and physical properties. Thus, it is suspected that the visual differences of EPS through SEM images could be due to the differing composition of the extracellular materials produced by *V. fischeri* and *E. coli*. Nevertheless, due to the small quantities of EPS produced by both bacterial species throughout this study, as well as limitations of the methods used for in situ EPS characterization, only tentative characterization of EPS is presented as inferred from the application of Concanavalin A. Further work concerning the clarification of the nature and chemical structure of EPS produced by both *V. fischeri* and *E. coli* is necessary in order to reasonably confirm the predictions discussed above.

Given that not only the substratum surface properties influence the initial bacterial attachment, bacterial surface characteristics have also been investigated. Bacteria are commonly found to exhibit a net negative charge (Hogt et al 1985; van Loosdrecht et al 1989; Sonohara et al 1995), the values of surface wettability and the negative zeta potential values obtained for *V. fischeri* and *E. coli* were similar to those published for other γ-proteobacteria (Li and Logan 2004). Both *V. fischeri* and *E. coli* possess negative surface charge ranging from –30 mV ± 9 mV to –38 mV ± 3 mV. It should be noted that the zeta potential measurements do not take into account the additional charge created by extracellular polymeric substances on the overall cell ensemble. Here, the zeta potential measurements were carried out to verify that the cellular surface characteristic were within an expected range rather than to predict adhesion tendencies. It is thought that Gram-negative bacteria have a negative charge due to the presence of certain major components of the outer membrane of the cell, for example; lipopolysaccharides (the carboxyl group carries a net negative charge), sialic acids and/or membrane proteins (Torimura et al 1999). Previous studies have recognized a negative correlation between bacterial cell electrokinetic properties and surface attachment (Li and Logan 2004). According to this consideration, both strains may have stronger affinity to the hydrophobic surfaces, eg, native P(*t*BMA). It also follows that the observed cellular charges of *V. fischeri* and *E. coli* predict that the slightly more negatively charged *E. coli* would be less likely to adhere to a surface in comparison to the slightly less negatively charged *V. fischeri.* In addition, *V. fischeri* cell surfaces appeared more hydrophobic. It is

likely that due to these strain characteristic differences, two studied bacteria exhibited expected strain-specific attachment pattern. However, both strains did not showed a strong affinity toward more hydrophobic native P(*t*BMA).

Since a few polymer surface characteristics have been modified, it was important to consider whether a particular parameter or a combination of all three parameters might positively influence attachment of *V. fischeri* and *E. coli*. Given that factors that have been identified to positively influence bacterial adhesion for some species include, eg, high surface hydrophobicity (Marshall et al 1971; Hogt et al 1983; Tegoulia and Cooper 2002), surface functionality (in particular, methyl groups) (Tegoulia and Cooper 2002) and significant topographical variation on the μm-scale (Characklis 1973; An et al 1995); native P(*t*BMA) would present a more attractive interface for bacterial adhesion in contrast to modified P(*t*BMA). In other words, the UV-irradiation of the native P(*t*BMA), as resulted in decreased surface hydrophobicity, replacement of methyl groups into carboxyl acid group, would lead in decreasing bacterial attachment. However, on the modified P(*t*BMA) surface, the average number of the bacterial cells was found to be greater. Therefore, it is suggested that the modification of surface roughness in the nanometer scale might trigger the elevated production of EPS and subsequent increase of attached bacterial cells. The results demonstrating enhanced bacterial attachment for nanosmooth polymer surfaces obtained in this study are in agreement with recently reported data on the impact of surface nanotopography on attachment of a marine bacterium *Pseudoalteromonas issachenkonii* on nanosmooth glass surfaces (Mitik-Dineva et al 2008). It was shown that the glass surface modification designed to achieve Rq of about 1.6 nm without any significant alteration of glass surfaces chemical composition and wettability, resulted in increase of bacterial attachment and alteration in cellular metabolic activity.

Conclusions

SEM analysis in combination with CSLM analysis revealed that both bacterial species, *V. fischeri* and *E. coli*, consistently showed a preference to adsorption onto the photolithographically modified P(*t*BMA) surface although the species-specific pattern of attachment was maintained. A decrease in P(*t*BMA) surface roughness upon UV-irradiation provided a nanosmooth surface, as well as an increase in the uniformity of surface characteristics. Despite alteration other surface characteristics such as hydrophobicity and surface chemistry, it is suggested that alternate factors such as surface nanometric topographical features may play an important role enhancing the bacterial adhesion process. In addition to obvious numerical differences, the bacterial metabolic response is changed as well. CSLM findings highlighted a large quantity of *V. fischeri*- and *E. coli*-associated EPS on the modified polymer surface. This is indicative of the surfaces modification strategy utilized by both strains to better sustain their existence on this surface. This observation implies that bacteria employ a 'simple' strategy for attachment to nanosmooth surfaces, by producing elevated amount EPS, although it is also possible that the presence of nanosmooth surfaces induces EPS production. A positive correlation between the presence of EPS and surface adhesion have been shown previously (Flemming and Wingender 2001; Kreft and Wimpenny 2001; Sutherland 2001), however, not in the context of surface nanotopography. The results of this study are of interest since they cast a doubt over the conventional notion that bacterial attachment is increased as the surface roughness increases on the μm – mm scale (Characklis 1973), and that ultra smooth surfaces would not encourage bacterial attachment (McAllister et al 1993). Although recent advances have transformed our understanding of bacterial interactions, we are still only beginning to appreciate the chemical and physical basis of cell-surface interactions. The application of nanotechnological tools to control the chemical and physical microenvironment surrounding cells will subsequently aid further research into enhancing our understanding of bacterial attachment behavior.

Acknowledgments

This study was supported in part by Australian Research Council (ARC) and RFBR 08-04-00099. The authors report no conflicts of interest in this work.

References

Abbot A, Rutter PR, Berkeley RC. 1983. The influence of ionic strength, pH and a protein layer of the interaction between *Streptococcus mutans* and glass surfaces. *J Gen Microbiol*, 129:439–45.

An YH, Friedman RJ. 1998. Consice review of mechanisms of bacterial adhesion to biomaterial surfaces. *J Biomed Mater Res Appl Biomater*, 43:338–48.

An YH, Friedman RJ, Draughn RA, et al. 1995. Rapid quantification of staphylococci adhered to titanium surfaces using image analyzed epifluorescence microscopy. *J Microbiol Methods*, 24:29–40.

Barth E, Myrvik QM, Wagner W, et al. 1989. *In vitro* and *in vivo* comparative colonization of *Staphylococcus aureus* and *Staphylococcus epidermidis* on orthopaedic implant materials. *Biomaterials*, 10:325–82.

Busscher HJ, Bos R, van der Mei HC, et al. 1999. Physico-chemistry of microbial adhesion from an overall approach to the limits. In: Baszkin A, Norde W (eds). *Physical Chemistry of Biological Interfaces*. New York: Marcel Dekker.

Busscher HJ, van der Mei HC. 1997. Physico-chemical interaction in initial microbial adhesion and relevance for biofilm formation. *Adv Dent Res*, 11:24–32.

Characklis WG. 1973. Attached microbial growths-II. Friction resistance due to microbial slimes. *Water Res*, 7:124–9.

Davey ME, O'Toole GA. 2000. Microbial biofilms: from ecology to molecular genetics. *Microbiol Mol Biol Rev*, 64:847–67.

de Kerchove AJ, Elimelech M. 2005. Relevance of electrokinetic theory for "soft" particles to bacterial cells: implication for bacterial adhesion. *Langmuir*, 21:6462–72.

Donlan RM. 2002. Biofilms: microbial life on surfaces. *Emerg Infect Dis*, 8:881–90.

Eboigbodin EK, Newton JR, Routh AF, et al. 2006. Bacterial quorum sensing and cell surface electrokinetic properties. *Appl Microbiol Biotechnol*, 73:669–75.

Eboigbodin KE, Newton JR, Routh AF, et al. 2005. Role of nonadsorbing polymers in bacterial aggregation. *Langmuir*, 21:12315–19.

Flemming HC, Wingender J. 2001. Relevance of microbial extracellular polymeric substances (EPSs) – Part I: Structural and ecological aspects. *Water Sci Technol*, 43:1–8.

Fletcher M. 1996. Bacterial attachment in aquatic environments: a diversity of surface and adhesion strategies, New York: Wiley-Liss.

Goldstein IJ, Hollerman CE, Smith EE. 1964. Protein-carbohydrate interaction. II. Inhibition studies on the interaction on concanavalin A with polysaccharides. *Biochemistry*, 4:876–83.

Gristina AG, Giridhar G, Gabriel BL, et al. 1993. Cell biology and molecular mechanism in artificial device infections. *Int J Artif Organs*, 16:755–64.

Handley PS, Rickard AH. 2001. Coaggreation – is it a universal biofilm phenomenon? In: Gilbert P, Allison DG, Brading M, et al. (ed). Biofilm Community Interactions: Chance or Necessity? Cardiff, UK: BioLine, pp. 1–10.

Harkes G, Feijen J. Darkez TY. 1991. Adhesion of *Escherichia coli* on to a series of poly(methacryates) differing in charge and hydrophobicity. *Biomaterials*, 12:853–60.

Hendricks SK, Kwok C, Shen M, et al. 1999. Plasma-deposited membranes for controlled release of antibiotic to prevent bacterial adhesion and biofilm formation. *J Biomed Mater Res*, 50:160–70.

Hogt AH, Dankert J, de Vries JA, et al. 1983. Adhesion of coagulase-negative staphylococci to biomaterials. *J Gen Microbiol*, 129:1959–68.

Hogt AH, Dankert J, Feijen J. 1985. Adhesion of *Staphylococcus epidermidis* and *Staphylococcus saprophyticus* to a Hydrophobic Material. *J Gen Microbiol*, 131:2485–91.

Hunter RJ. 1995. Foundations of Colloid Science, New York: Oxford: Clarendon Press.

Invitrogen. 2006. Vybrant® CFDA SE Cell Tracer Kit [online]. Accessed on April 3, 2008. URL: http://www.probes.invitrogen.com/.

Ivanova EP, Alexeeva YV, Pham DK, et al. 2006. ATP level variations in heterotrophic bacteria during attachment on hydrophilic and hydrophobic surfaces. *Int Microbiol*, 9:37–46.

Ivanova EP, Wright JP, Pham DK, et al. 2006. A comparative study between the adsorption and covalent binding of human immunoglobin and lysozyme on surface-modified poly(tert-butyl methacrylate). *Biomed Mater*, 1:24–32.

Kreft JU, Wimpenny JW. 2001. Effect of EPS on biofilm structure and function as revealed by an individual-based model of biofilm growth. *Water Sci Technol*, 43:135–41.

Krieg NR, Holt JG. 1984. Bergey's Manual of Bacteriology. Philadelphia, PA: Lippincott Williams and Wilkins.

Li B, Logan BE. 2004. Bacterial adhesion to glass and metal-oxide surfaces. *Colloids Surf B Biointerfaces*, 36:81–90.

Liang MN, Smith SP, Metallo SJ, et al. 2000. Measuring the forces involved in polyvalent adhesion of uropathogenic *Escherichia coli* to mannose-presenting surfaces. *Proc Natl Acad Sci U S A*, 97:13092–6.

Loeb GI, Neihof RA. 1975. Marine conditioning films. *Adv Chem*, 145:319–35.

Marsh PD, Bradshaw DJ. 1997. Physiological approaches to the control of oral biofilms. *Adv Dent Res*, 11:176–85.

Marshall KC. 1984. Microbial adhesion and aggregation. Report of the Dahlem Workshop on Microbial Adhesion and Aggregation Berlin 1984. New York: Springer.

Marshall KC, Stout R, Mitchell R. 1971. Mechanism of the initial events in the sorption of marine bacteria to surfaces. *J Gen Microbiol*, 68:337.

Masliyah JH. 1994. Electrokinetic transport phenomena. Edmonton, Canada: AOSTRA.

McAllister EW, Carey LC, Brady PG, et al. 1993. The role of polymeric surface smoothness of biliary stents in bacteria adhesion, biofilm deposition and stent occlusion. *Gastrointest Endosc*, 39:422–5.

Mitik-Dineva N, Wang J, Mocanasu RC, et al. 2008. Impact of nano-topography on bacterial attachment. *Biotechnol J*, 3:1–9.

Oga M, Sugioka Y, Hobgood CD, et al. 1988. Surgical biomaterial and differential colonization by *Staphylococcus epidermidis. Biomaterials*, 9:285–9.

Percival SL, Walker JT, Hunter PR. 2000. Microbiological aspect of biofilms and drinking water. Baton Rouge, LA: CRC Press.

Pham DK, Invanova EP, Wright, DP, et al. 2003. AFM analysis of the extracellular polymeric substances (EPS) released during bacterial attachment on polymeric surfaces. *Manipulation and Analysis of Biomoleucles*, *Cells and Tissues*, 4962:151–9.

Pringle JH, Fletcher M. 1986. Influence of substratum hydration and adsorbed macromolecules on bacterial attachment to surfaces. *Appl Environ Microbiol*, 51:1321–5.

Reynolds EC, Wong A. 1983. Effect of adsorbed protein on hydroxyapatite zeta potential and *Streptococcus mutans* adherance. *Infect Immun*, 39:1285–90.

Sambrook J, Russell DW. 2001. Molecular cloning: A laboratory manual. 3rd Ed. Cold Spring Habor, New York: Cold Spring Habor Laboratory.

Senaratne W, Adnruzzi L, Ober CK. 2005. Self-assembled monolayers and polymer brushes in biotechnology: current applications and future perspectives. *Biomacromolecules*, 6:2427–48.

Sonohara R, Muramatsu N, Ohshima H, et al. 1995. Difference in surface properties between *Escherichia coli* and *Staphylococcus aureus* as revealed by electrophoretic mobility measurements. *Biophys Chem*, 55:273–7.

Stoodley P, Sauer K, Davies DG, et al. 2002. Biofilms as complex differentiated communities. *Ann Rev Microbiol*, 56:187–209.

Sutherland IW. 2001. Exopolysaccharides in Biofilms, Flocs and Related Structures. *Water Sci Technol*, 43:77–86.

Tegoulia VA, Cooper SL. 2002. *Staphylococcus aureus* adhesion to self-assembled monolayers: effect of surface chemistry and fibrinogen presence. *Colloids Surf B Biointerfaces*, 24:217–28.

Torimura M, Ito S, Kano K, et al. 1999. Surface characterization and on-line activity measurements of microorganisms by capillary zone electrophoresis. *J Chromatogr B Biomed Sci Appl*, 721:31–7.

Tsuneda S, Aikawa H, Hayashi H, et al. 2004. Significance of cell electrokinetic properties determined by soft-particle analysis in bacterial adhesion onto a solid surface. *J Colloid Interface Sci*, 279:410–7.

Tsuneda S, Jung J, Aikawa H, et al. 2003. Influence of extracellular polymers on electrokinetic properties of heterotrophic bacterial cells examined by soft particle electrophoresis theory. *Colloids Surf B Biointerfaces*, 29:181–8.

van Loosdrecht MCM, Lyklemea J, Norde W, et al. 1989. Bacterial adhesion: a physicochemical approach. *Microb Ecol*, 17:1–15.

Waar K, van der Mei HC, Degener JE, et al. 2002. *Enterococcus faecalis* surface proteins determine its adhesion mechanism to bile drain materials. *Microbiology*, 148:1863–70.

Watnick PI, Kolter R. 1999. Steps in the development of a Vibrio cholerae biofilm. *Mol Microbiol*, 34:586–95.

Weibel DB, DiLuzio WR, Whitesides GM. 2007. Microfabrication meets microbiology. *Nature Rev Microbiol*, 5:209–18.

Wozniak DJ, Wyckoff TJ, Starkey M, et al. 2003. Alginate is not a significant component of the extracellular polysaccharide matrix of PA14 and PAO1 *Pseudomonas aeruginosa* biofilms. *Proc Natl Acad Sci U S A*, 100:7907–12.

Wright AC, Simpson LM, Oliver JD, et al. 1990. Phenotypic evaluation of a capsular transposon mutants of Vibrio vulnificus. *Infect Immun*, 58:1769–73.

Yildiz FH, Schoolnik GK. 1999. *Vibrio cholerae* O1 E1 Tor: Identification of a gene cluster required for the rugose colony type; exopolysaccharide production, chlorine resistance, and biofilm formation. *Proc Natl Acad Sci U S A*, 96:4028–33.

Zobell CE. 1937. The influence of solid surfaces upon the physiological activities of bacteria in sea water. *J Bacteriol*, 33:86.

Zobell CE. 1942. The effects of solid substrate surfaces upon bacterial activity. *J Bacteriol*, 46:39–56.

Zobell CE, Allen EC. 1935. The significance of marine bacteria in the fouling of submerged surfaces. *J Bacteriol*, 29:239–51.